An age–colour relationship for main-belt S-complex asteroids

Robert Jedicke[1], **David Nesvorný**[2], **Robert Whiteley**[3], **Željko Ivezić**[4] **& Mario Jurić**[4]

[1]*Institute for Astronomy, University of Hawaii, Honolulu, Hawaii 96822, USA*
[2]*Southwest Research Institute, 1050 Walnut St, Suite 400, Boulder, Colorado 80302, USA*
[3]*USAF Space and Missile Systems Center, 2420 Vela Way, Suite 146, Los Angeles Air Force Base, El Segundo, California 90245, USA*
[4]*Princeton University, Department of Astrophysical Sciences, Princeton, New Jersey 08544, USA*

Asteroid collisions in the main belt eject fragments that may eventually land on Earth as meteorites[1–3]. It has therefore been a long-standing puzzle in planetary science that laboratory spectra of the most populous class of meteorite (ordinary chondrites, OC) do not match the remotely observed surface spectra of their presumed (S-complex) asteroidal parent bodies. One of the proposed solutions to this perplexing observation is that 'space weathering' modifies the exposed planetary surfaces over time through a variety of processes (such as solar and cosmic ray bombardment, micro-meteorite bombardment, and so on). Space weathering has been observed on lunar samples[4], in Earth-based laboratory experiments[5,6], and there is good evidence from spacecraft data that the process is active on asteroid surfaces[7,8]. Here, we present a measurement of the rate of space weathering on S-complex main-belt asteroids using a relationship between the ages of asteroid families and their colours[9]. Extrapolating this age–colour relationship to very young ages yields a good match to the colour of freshly cut OC meteorite samples, lending strong support to a genetic relationship between them and the S-complex asteroids.

Neither laboratory nor spacecraft measurements have measured the rate of space weathering on asteroids. In the laboratory it is difficult to calibrate the techniques used in simulating the process (for example, rapid laser heating of crushed OC meteorite samples[5–6]) with the presumed actual mechanism (micro-meteoroid-induced heating of regolith grains). Estimates of characteristic time scales[6,10] for asteroidal space weathering based on laboratory results vary from 5×10^4 yr to 10^8 yr. From the spacecraft's vantage point it is possible to distinguish young from old terrains on the basis of crater counting or other geological morphology (for example, rock slides) but it is difficult to date the surface's absolute ages, because cratering rates on asteroid surfaces vary with time, orbital elements, size and so on. Space weathering on Eros seems to reach maturity on timescales of several tens of millions of years (C. R. Chapman, unpublished work).

We have developed a technique for measuring the rate of space weathering on main-belt asteroids (Fig. 1). Our method uses asteroid families that are genetically related groups of objects that were created in the collisional disruption of a larger asteroid. The surfaces of asteroids in a family must all have the same age as they are all 're-set' by the catastrophic disruption that generated the group. When the collision takes place, many large fragments are ejected and they re-accumulate a layer of material on their surfaces that was formerly in the interior of the parent asteroid[11]. The identification of asteroid families and determination of their ages is described in Supplementary Information.

We obtained asteroid colours from the Sloan Digital Sky Survey Moving Object Catalog[9] (SDSS MOC) that contains 5-band (u,g,r,i,z) photometric data accurate to 0.02 magnitudes for over 135,000 entries. More than 28,000 were linked to known asteroids with proper elements from the AstDys database[12]. Because our

identification of asteroid families was performed on the same set of proper elements, we were able to cross-link 8,416 asteroids with a known family identification to the MOC. Twelve of the families are classified unambiguously as S-complex by other researchers and/or are well determined by the colours from the MOC itself as described in Supplementary Information.

Although the classification of our families as members of the S-complex is well determined, there are many subtypes within this broad taxonomic complex. In particular, a classification scheme based on mineralogical absorption features[13] in the infrared suggests that only one subclass (SIV) is mineralogically consistent with an OC meteorite connection. We will argue below that our results suggest that there is a space-weathering connection between S-complex asteroids and the OC meteorites, and it would therefore seem that this analysis should be restricted to only those families of the SIV sub-type. There are two problems with this option: (1) the mineralogical classification scheme has been applied to only 39 asteroids, and only two of those objects are among the thousands of asteroids in our family members, and (2) that classification scheme ignored the possibility of space weathering, assigning all the variability within the S-complex to mineralogical diversification. Similarly, the Eos family contains many K-type (a subclassification within the S-complex) asteroids that are thought to be related to the CO3 or CV3 chondrites rather than the OC meteorites[14].

This study shows that there is an age-dependent component to asteroid colours along with mineralogical differences. As we have no *a priori* means of disentangling these effects, we make no distinction between families of different types within the S-complex. Furthermore, in the wavelength range of the SDSS filters, there are few features available to distinguish quantitatively between S-complex asteroids except for the slope that is related to the first principal component (PC_1) colour shown in Fig. 1.
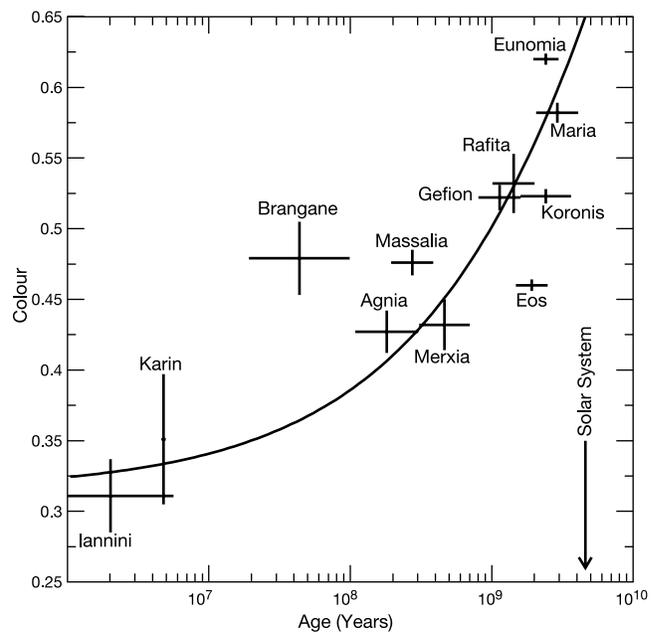

Figure 1 The relationship between the mean colour of S-complex asteroid families and their ages. The PC_1 colour captures ~73% of the variance in colours between asteroids with good spectrophotometric measurements ($\Delta PC_1 < 0.1$) in the SDSS MOC. It is a good proxy for the mean spectral slope between 350 nm and 900 nm. Larger values of PC_1 correspond to higher slopes (redder objects) in that wavelength range. The PC_1 for a family is the standard weighted mean of all measured values for the members of the family. The displayed error bars on PC_1 are the standard error of the weighted mean colour. The solid line represents a fit to the data points accounting for errors in both the ordinate and abscissa.

We used u–g, g–r, g–i and g–z colour bands for 10,776 objects culled from the entire MOC with photometric errors in each band of less than 0.10 magnitudes as input to a principal components (PC) analysis[15] that creates mutually orthogonal linear combinations (eigenvectors) of the colours. In doing so it collapses the input data into successive components that incorporate the maximum remaining variance of the colours. It thus provides a measure of the true dimensionality of the input system so that we can concentrate our efforts on the most important colour terms. We found that ~73% of the variation in the colours is incorporated into $PC_1 = 0.3560 m_{ug} + 0.5418 m_{gr} + 0.5683 m_{gi} + 0.5066 m_{gz}$, where m_{xy} is the x–y colour for the asteroid after correction for solar colours [$m_{xy} = (m_x - m_y)_{SDSS} - (m_x - m_y)_{Sun}$]. We have found that PC_1 is well correlated with the slope of the reflectance spectrum in the wavelength range of 350 nm to 900 nm, and is thus a good measure of the reddening effect caused by space weathering. PC_1 is also well correlated with the SDSS colour components[16].

Figure 1 shows that PC_1 depends on a family's age. Assuming that the change in colour is related to the amount of asteroid surface processed by a constant flux of a space-weathering agent, we expect the change of colour as a function of time to be given by $PC_1(t) = PC_1(0) + \Delta PC_1\{1 - \exp[-(t/\tau)]\}$. We have generalized the form to $PC_1(t) = PC_1(0) + \Delta PC_1\{1 - \exp[-(t/\tau)^\alpha]\}$ for the fit shown on the figure with $PC_1(0) = 0.32 \pm 0.01$, $\Delta PC_1 = 1.0 \pm 0.1$, $\tau = (25 \pm 5) \times 10^9$ years and $\alpha = 0.50 \pm 0.05$.

The characteristic timescale for space-weathering is $\tau = 10^{10.4 \pm 0.2}$ years, which is two orders of magnitude larger than estimates (~10^8 years) based on laboratory measurements of laser-induced simulated weathering of ground meteoritic samples[6] intended to simulate the effects of micro-meteoroid bombardment. Interaction of the solar wind with asteroid surfaces is predicted[10] to alter them much faster, perhaps within a characteristic timescale of only ~$10^{4.7}$ years.

The caveat is that with existing data our technique is insensitive to measurements of subcomponents of the space-weathering process (for example, there might exist a fast and slow mechanism) if it occurs on timescales of <~10^6 years because it would require a sample of very young families (for example, 10^2–10^5 years) with well-measured colours. Other known effects of space weathering include spectrum-wide darkening and a reduction in the band depths of absorption features. We were not able to identify any significant change as a function of time in the SIMPS[17] albedo or 2MASS J/H and K/H infrared-band ratios[18] for the S-complex families. This might be due to a lack of sensitivity of our technique (for example, space weathering occurring too fast) and could indicate that different processes act at varying timescales to create the overall space-weathering phenomenon. It is also possible that gardening of the surface regolith through regular bombardment by small asteroids could significantly lengthen the effective space-weathering timescale[10] on the basis of laboratory experiments.

Meteorite spectra in the laboratory are obtained from freshly exposed (ground or crushed) surfaces and therefore correspond to the surface ages of newly formed asteroid families. We predict that the mean PC_1 for new families should be 0.32 ± 0.01, whereas families formed at the beginning of the Solar System ~4.650×10^9 years ago should have $PC_1 = 0.67 \pm 0.07$, as shown on Fig. 2. The age–colour correlation presented here, along with a contribution from intrinsic mineralogical differences between the parent bodies, can explain the observation of colour diversity between families[16] within the S-complex.

The mean PC_1 for the OC meteorites in Fig. 2 is 0.39 ± 0.10 (the mean is 0.36 ± 0.06 without the LL3 subclass—with $PC_1 \approx 0.59$ its colours are already similar to the S-complex's). Our prediction for the unweathered colour of S-complex asteroids agrees well with the observed mean PC_1 for the OC meteorites. Our prediction for S-complex asteroid surfaces with an age equal to that of the Solar System is slightly higher than the mean colour of all S-complex asteroids, as would be expected if the majority have experienced some space-weathering. The mode colour of the S-complex asteroids (0.557 ± 0.004) corresponds to an asteroid that has aged for ~1.9×10^9 years.

Our result, along with a growing body of indirect evidence, strongly supports earlier speculation[7] that most S-complex asteroids could be OC meteorite parent bodies. Asteroid spectra with typical OC meteorite features are known as Q-types, as exemplified by (1862) Apollo. Even though there is little to no remote-sensing evidence[7] of Q-type asteroids in the main belt, all four S-complex asteroids for which in situ measurements exist (Gaspra, Ida, Dactyl, Eros) have surfaces that are more OC-like in recently excavated terrain leading to the conclusion (C. R. Chapman, unpublished work) that all four are probably OC bodies.

Assuming that S-complex asteroids are the OC parent bodies, our determination of the space-weathering rate correctly predicts the colour of fresh ordinary chondritic material. We predict that as spectroscopists are able to image smaller main-belt asteroids they will increasingly find them to be more Q- or OC-like. Indeed the SMASS2 survey[19] finds some main-belt spectra verging towards Q-type. However, even larger main-belt S-complex asteroids such as (6) Hebe, often cited as a possible OC parent body, can produce OC meteorites. Observations of rotationally resolved spectroscopic heterogeneity[20] on that asteroid may be the result of varying degrees of space weathering on different hemispheres.

Given the rate at which main-belt asteroid families are produced, and the distribution of dynamical times for evolution onto Earth-crossing orbits, our results can predict the ratio of Q- to S-type asteroids in the main belt and amongst the near-Earth object (NEO) population. Main-belt S-type asteroids will produce S-type progeny whose freshly exposed surfaces should exhibit Q- or OC-like spectra
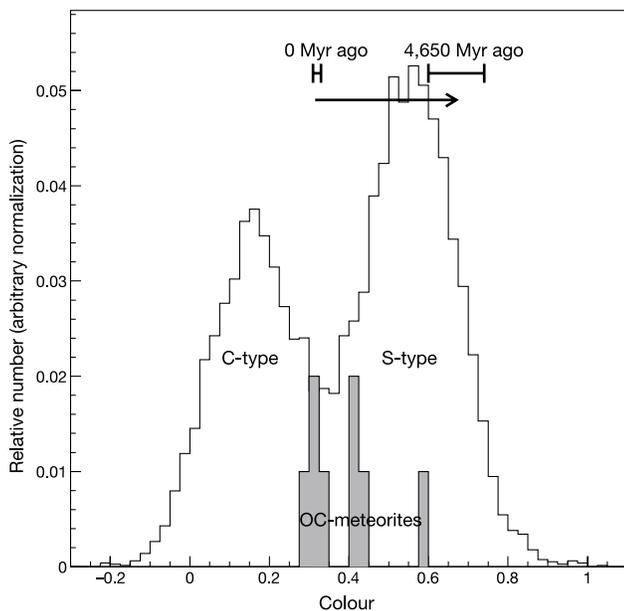

Figure 2 The distribution of colours for S- and C-complex asteroids detected by the SDSS and the average colours of eight types of ordinary chondrite meteorites. Normalized PC_1 distribution for SDSS MOC entries with $\Delta PC_1 < 0.1$ (solid line) and OC meteorites (filled histogram). The peak on the right is the S-complex of asteroids and the peak on the left the C-complex. A gaussian fit to the S-complex PC_1 (>0.45) distribution yields the most likely S-complex $PC_1 = 0.557 \pm 0.004$. We used the average OC spectra for (from left to right in the histogram) H5, L6 (type i), LL6, H6, L4, L6 (type ii), L5 and LL3 meteorites of ref. 27 convolved with the solar spectrum and the SDSS system transmission then transformed to PC_1. PC_1 ranges indicated by error bars at the top are predictions for new and old ($4,650 \times 10^6$ years) S-complex material. The arrow points from the central prediction for each in the direction of increased ageing.

after cratering events and catastrophic disruptions. The newly created object's orbits will gradually evolve and perhaps be transported into one of the strong resonances that can pump the orbit's eccentricity to Earth-crossing values. Smaller objects will migrate faster under the influence of the Yarkovsky effect[21], and once in a resonance the dynamical lifetime of objects of any size is of the order of only a few million years[2]. However, cosmic ray exposure ages tell us that most OC meteorites are tens of millions of years old[22]. This indicates that even the smallest meteoroids spend a considerable amount of time migrating from their point of origin into the resonances, and the larger objects that eventually become NEOs probably require even more time. Thus, we expect that NEOs of S-complex provenance will display a size-dependent range of spectra ranging from Q (or OC) to S. This prediction is supported by numerous reports in the past decade indicating Q-like spectra and a size-dependent trend to OC-like spectra with decreasing size in the NEO population[23–26]. However, space weathering in the main belt occurs faster than the lifetimes of NEOs, as suggested by meteoritic cosmic ray exposure ages[22]. Thus, observational evidence for a large number of OC-like spectra amongst the NEOs[23–26] implies that regular re-surfacing of these objects keep them looking younger longer. □

1. Vokrouhlický, D. & Farinella, P. Efficient delivery of meteorites to the Earth from a wide range of asteroid parent bodies. *Nature* **407,** 606–608 (2000).
2. Gladman, B. J. *et al.* Dynamical lifetimes of objects injected into asteroid belt resonances. *Science* **277,** 197–201 (1997).
3. Wisdom, J. Meteorites may follow a chaotic route to earth. *Nature* **315,** 731–733 (1985).
4. Adams, J. B. & McCord, T. B. Alteration of lunar optical properties: Age and composition effects. *Science* **171,** 567–571 (1971).
5. Moroz, L. V., Fisenko, A. V., Semjonova, L. F., Pieters, C. M. & Korotaeva, N. N. Optical effects of regolith processes on S-asteroids as simulated by laser shots on ordinary chondrite and other mafic materials. *Icarus* **122,** 366–382 (1996).
6. Sasaki, S., Nakamura, K., Hamabe, Y., Kurahashi, E. & Hiroi, T. Production of iron nanoparticles by laser irradiation in a simulation of lunar-like space weathering. *Nature* **410,** 555–557 (2001).
7. Chapman, C. R. S-type asteroids, ordinary chondrites, and space weathering: The evidence from Galileo's fly-bys of Gaspra and Ida. *Meteorit. Planet. Sci.* **31,** 699–725 (1996).
8. Clark, B. E. *et al.* Space weathering on Eros: Constraints from albedo and spectral measurements of Psyche crater. *Meteorit. Planet. Sci.* **36,** 1617–1637 (2001).
9. Ivezić, Ž., Jurić, M., Lupton, R. H., Tabachnik, S. & Quinn, T. in *Survey and Other Telescope Technologies and Discoveries* (eds Tyson, J. A. & Wolff, S.) Vol. 4836, 98–103 *Proc. SPIE* (2002).
10. Hapke, B. Space weathering from Mercury to the asteroid belt. *J. Geophys. Res.* **106,** 10039–10074 (2001).
11. Michel, P., Benz, W., Tanga, P. & Richardson, D. C. Collisions and gravitational reaccumulation: Forming asteroid families and satellites. *Science* **294,** 1696–1700 (2001).
12. Milani, A. & Knežević, Z. Asteroid proper elements and the dynamical structure of the asteroid main belt. *Icarus* **107,** 219–254 (1994).
13. Gaffey, M. J. *et al.* Mineralogical variations within the S-type asteroid class. *Icarus* **106,** 573–602 (1993).
14. Doressoundiram, A., Barucci, M. A., Fulchignoni, M. & Florczak, M. EOS family: A spectroscopic study. *Icarus* **131,** 15–31 (1998).
15. Deeming, T. J. Stellar spectral classification, I. *Mon. Not. R. Astron. Soc.* **127,** 493–516 (1964).
16. Ivezić, Ž. *et al.* Color confirmation of asteroid families. *Astron. J.* **124,** 2943–2948 (2002).
17. Tedesco, E. F., Noah, P. V., Noah, M. & Price, S. D. The supplemental IRAS minor planet survey. *Astron. J.* **123,** 1056–1085 (2002).
18. Sykes, M. V. *et al.* The 2MASS asteroid and comet survey. *Icarus* **146,** 161–175 (2000).
19. Bus, S. J. & Binzel, R. P. Phase II of the small main-belt asteroid spectroscopic survey. *Icarus* **158,** 106–145 (2002).
20. Migliorini, F. *et al.* Surface properties of (6) Hebe: A possible parent body of ordinary chondrites. *Icarus* **128,** 104–113 (1997).
21. Morbidelli, A. & Vokrouhlický, D. The Yarkovsky-driven origin of near-Earth asteroids. *Icarus* **163,** 120–134 (2003).
22. Marti, K. & Graf, T. Cosmic-ray exposure history of ordinary chondrites. *Annu. Rev. Earth Planet. Sci.* **20,** 221–243 (1992).
23. Binzel, R. P., Bus, S. J., Burbine, T. H. & Sunshine, J. M. Spectral properties of near-Earth asteroids: evidence for sources of ordinary chondrite meteorites. *Science* **273,** 946–948 (1996).
24. Rabinowitz, D. L. Size and orbit dependent trends in the reflectance colours of earth-approaching asteroids. *Icarus* **134,** 342–346 (1998).
25. di Martino, M., Manara, A. & Migliorini, F. 1993 VW: an ordinary chondrite-like near-Earth asteroid. *Astron. Astrophys.* **302,** 609–612 (1995).
26. Lazzarin, M., di Martino, M., Barucci, M. A., Doressoundiram, A. & Florczak, M. Compositional properties of near-Earth asteroids: spectroscopic comparison with ordinary chondrite meteorites. *Astron. Astrophys.* **327,** 388–391 (1997).
27. Gaffey, M. J. Spectral reflectance characteristics of the meteorite classes. *J. Geophys. Res.* **81,** 905–920 (1976).

....

Tonks–Girardeau gas of ultracold atoms in an optical lattice

Belén Paredes[1], **Artur Widera**[1,2,3], **Valentin Murg**[1], **Olaf Mandel**[1,2,3], **Simon Fölling**[1,2,3], **Ignacio Cirac**[1], **Gora V. Shlyapnikov**[4], **Theodor W. Hänsch**[1,2] & **Immanuel Bloch**[1,2,3]

[1]*Max-Planck-Institut für Quantenoptik, D-85748 Garching, Germany*
[2]*Sektion Physik, Ludwig-Maximilians-Universität, Schellingstrasse 4/III, D-80799 Munich, Germany*
[3]*Institut für Physik, Johannes Gutenberg-Universität, D-55099 Mainz, Germany*
[4]*Laboratoire Physique Théorique et Modèles Statistique, Université Paris Sud, Bâtiment 100, 91405 Orsay Cedex, France, and Van der Waals-Zeeman Institute, University of Amsterdam, 1018 XE Amsterdam, The Netherlands*

....

Strongly correlated quantum systems are among the most intriguing and fundamental systems in physics. One such example is the Tonks–Girardeau gas[1,2], proposed about 40 years ago, but until now lacking experimental realization; in such a gas, the repulsive interactions between bosonic particles confined to one dimension dominate the physics of the system. In order to minimize their mutual repulsion, the bosons are prevented from occupying the same position in space. This mimics the Pauli exclusion principle for fermions, causing the bosonic particles to exhibit fermionic properties[1,2]. However, such bosons do not exhibit completely ideal fermionic (or bosonic) quantum behaviour; for example, this is reflected in their characteristic momentum distribution[3]. Here we report the preparation of a Tonks–Girardeau gas of ultracold rubidium atoms held in a two-dimensional optical lattice formed by two orthogonal standing waves. The addition of a third, shallower lattice potential along the long axis of the quantum gases allows us to enter the Tonks–Girardeau regime by increasing the atoms' effective mass and thereby enhancing the role of interactions. We make a theoretical prediction of the momentum distribution based on an approach in which trapped bosons acquire fermionic properties, finding that it agrees closely with the measured distribution.

The physics of ultracold one-dimensional (1D) Bose systems is very different from that of ordinary three-dimensional (3D) cold gases[1,2,4,5]. For example, by decreasing the particle density n, a usual 3D quantum many-body system becomes more ideal, whereas in a 1D Bose gas the role of interactions becomes more important. The reason is that at temperatures $T \to 0$, the kinetic energy of a particle at the mean interparticle separation is $K \propto n^2$ and it decreases with decreasing density n faster than the interaction energy per particle, $I \propto n$. The ratio of the interaction to kinetic energy, $\gamma = I/K$, characterizes the different physical regimes of the 1D quantum gas. For a large value of γ, the gas enters the Tonks–Girardeau (TG) regime, where the repulsion between particles strongly decreases the wavefunction at short interparticle distances.

Achieving such a TG regime and observing 'fermionization' of